Available online at www.sciencedirect.com
SCIENCE DIRECT®
Physica C 400 (2004) 97–104
PHYSICA C
www.elsevier.com/locate/physc

Study of the sintering behaviour of MgB_2 superconductor during hot-pressing

A. Tampieri [a,*], G. Celotti [a], S. Sprio [a,*], R. Caciuffo [b,c], D. Rinaldi [b,c]

[a] *ISTEC-CNR, Via Granarolo 64, 48018 Faenza (RA), Italy*
[b] *FIMET, University of Ancona, Via Brecce Bianche, 60131 Ancona, Italy*
[c] *INFM, Unità di Ancona, Italy*

Received 15 July 2003; received in revised form 15 July 2003; accepted 16 July 2003

Abstract

The densification behaviour of MgB_2 was studied when commercial powder was hot-pressed in the temperature range 1070–1190 °C. The mechanisms active during sintering were investigated by continuously recording the shrinkage vs. time and elaborating the data on the basis of Kingery's model for liquid phase sintering. XRD and SEM analysis on final dense bodies were used to evaluate secondary phases formation during sintering and the effect of magnesium sublimation. AC magnetic susceptibility measurements were also performed to correlate the microstructural and morphological modifications induced by hot-pressing and the superconducting properties.

Keywords: MgB_2; Hot pressing; Kingery's model

1. Introduction

The discovery of superconductivity in MgB_2 [1] has aroused a great interest and many efforts are presently carried out to check its applicability in the realisation of devices, especially by improving its transport current, which is strongly affected by the phase purity and density.

MgB_2 is currently synthesised by a classical solid state reaction between elemental reactants, obtaining almost pure superconducting phase; anyway the normal synthesis route does not allow to obtain dense samples because of Mg evaporation above 800 °C. To overcome this problem, various pressure sintering techniques have been applied to densify the superconductor and make it suitable for technological applications. Hot-pressing and hot deformation techniques [2–4] has been reported to densify the material up to full density and to induce a weak *c*-axis alignment along the pressure direction. At the same way reactive sintering has been attempted by hot isostatic pressing (HIP) [1,7] at 196 MPa and 700 °C yielding 50% pure MgB_2 phase in 10 h. In the case of high pressure synthesis [5,6] (3–5 GPa at 900–1000 °C) the percentage of MgB_2 obtained is much higher (around 90%) and relative density reaches 100%.

In this paper the study of the densification behaviour of MgB_2 during hot-pressing has been

* Corresponding authors. Tel.: +39-546699711; fax: +39-54646381.
E-mail address: sprio@istec.cnr.it (S. Sprio).

0921-4534/$ - see front matter © 2003 Elsevier B.V. All rights reserved.
doi:10.1016/S0921-4534(03)01310-8

evaluated starting form commercial MgB_2 powder and the densification curves, obtained at different sintering temperatures in isothermal regime, interpreted on the basis of Kingery's model.

2. Experimental

MgB_2 commercial powder (Alfa Aesar) was used for hot-pressing experiments. Its purity was checked by XRD (Miniflex, Rigaku, CuKα radiation); specific surface and particle size distribution were evaluated by BET technique (FlowSorb II 2300, Micromeritics) and X-ray sedimentography (Sedigraph 5100, Micromeritics) respectively.

About 25 g of powder were put in a graphite die and positioned into the furnace; afterwards the chamber was evacuated and the sample heated until the final sintering temperature; a first experiment was performed, in order to find the starting temperature for sintering; it was found that densification starts at $T = 1050$ °C. Afterwards, five different samples were prepared with different sintering temperatures: 1070, 1100, 1130, 1160 and 1190 °C. During each experiment the hot-pressing temperature was reached with a ramp rate of 10/°C and at $T = 500$ °C a pressure of 30 MPa was applied by a graphite punch. The sample was kept at the final sintering temperature for 20 min and then spontaneously cooled under vacuum until ambient temperature (the hot-pressing cycle is reported in Fig. 1). The shrinkage was continuously recorded. The MgB_2 piece was extracted, sectioned perpendicularly to the direction of pressing by using a low-speed oil cooled wheel and observed by XRD to check the phase purity; density measurements were made by Archimede's and geometric method. SEM observations (Leica, Cambridge) were performed on sintered pieces on polished and fractured samples. The study of the possible sintering mechanisms and their kinetics was performed by plotting $\Delta L/L_0$ vs. time in a log–log scale (where $\Delta L = L_0 - L$, with $L_0 =$ initial sample thickness and L the recorded sample thickness during hot-pressing cycle).

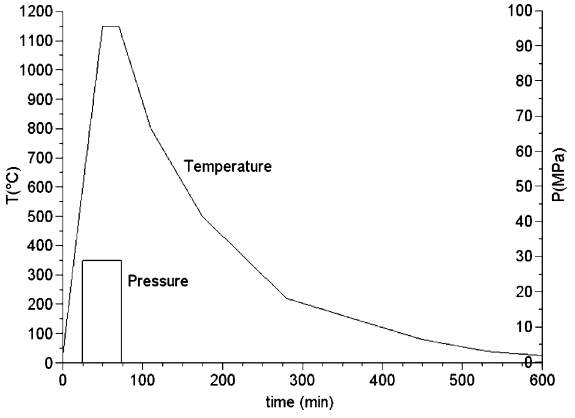

Fig. 1. Hot-pressing cycle.

In these plots the curves become broken lines, whose branches identify a specific sintering mechanism, according to the Kingery's model for liquid phase sintering [8,9]. The slope of each branch was found by linear regression on all experimental points. Finally, magnetic ac susceptibility measurements were performed on suitably shaped pieces of the sintered samples (about $2\times2\times12$ mm) by using a commercial mutual inductance Quantum Design susceptometer, collecting data with a driving field amplitude varying from $H_{ac} \approx 10$ A/m to $H_{ac} \approx 1200$ A/m, oscillating at a frequency of 1000 Hz, on warming from 15 K after zero-field cooling of the samples. Some measurements were repeated with a commercial Lake Shore susceptometer as a check.

3. Results and discussion

The commercial powder was characterized by SEM: in Fig. 2 elongated grains as small as 150–200 nm are visible and an average size of primary particles around 500–600 nm can be estimated. On the other hand mean particle size, determined by sedimentography turned out to be $\approx$10 μm which is the dimension of particle agglomerates not completely disgregated by the ultrasound treatment. Specific surface area determined by BET resulted 3.57 m^2/g, which corresponds to a mean primary particle size of about 0.65 μm in good agreement with SEM analysis.

XRD analysis shows that starting powder is composed by MgB_2 and about 3 vol.% of MgO.

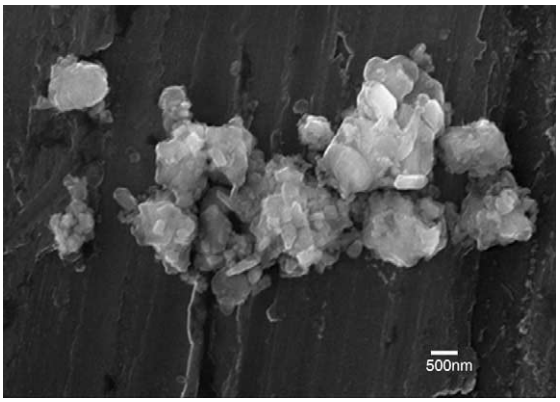

Fig. 2. SEM image of MgB_2 starting powder.

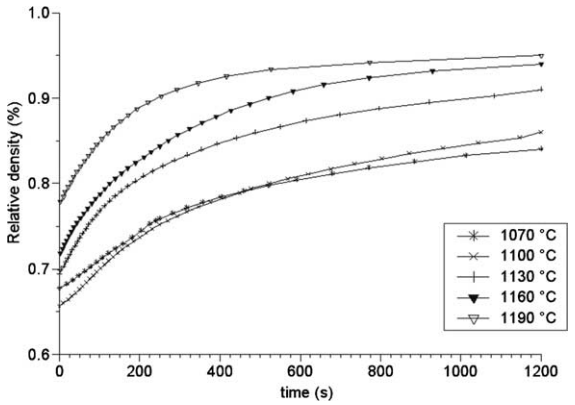

Fig. 3. Densification vs. time curves of hot-pressed MgB_2 at different temperatures.

First attempts to densify MgB_2 by hot-pressing showed that the shrinkage was detectable starting from $T \approx 1050$ °C, therefore densification experiments were performed in the range 1070–1190 °C. The study of the isothermal densification curves recorded during hot-pressing at different temperatures (Fig. 3) reveals that samples treated at 1070, 1100 and 1130 °C have a very similar densification behaviour, with the exception of the curve at 1070 °C which reaches higher densification extent during heating up and thus starts the isothermal permanence at higher density value.

At temperatures higher than 1130 °C the curves show a different shape due to the lack of an induction period (which occurs during the heating up); in particular the curve obtained at 1190 °C shows a steep slope followed by a marked plateau. Mg sublimation, expected to start at ≈800 °C [10], is delayed by the applied pressure and starts to occur at about 1000 °C causing the formation of MgB_4 and MgO which probably forms during cooling, through the oxidation of Mg trapped into pores. Mg vaporization was checked on MgB_2 green pellets subjected to TG–DTA analysis in argon atmosphere showing the occurrence of two phenomena: oxidation (starting at $T \approx 300$ °C) and vaporization of Mg. Exploiting XRD data recorded on the pellet after thermal analysis it was possible to isolate the contribution of weight loss due to vaporization, which starts at about 800 °C [10]. From XRD data (Table 1) it can be seen that the amount of secondary phases and Mg loss slightly increase with temperature, while they are strongly influenced by sintering time: the formation of borides with a smaller Mg/B ratio, like MgB_6 and MgB_{12}, occurs more and more for sintering time higher than 20 min in agreement with previous data on MgB_2 thermal decomposition [10].

Table 1
Phase composition (vol.%) of MgB_2 hot-pressed for 20 min at different temperatures

	1070	1100	1130	1160	1190
MgB_2	90	85.5	85.5	85.5	85.5
MgO	8.5	13	13	13	13
MgB_4	1.5	1.5	1.5	1.5	1.5
Mg loss (wt.%)	1	1	1.5	2	2

The densification curves have been interpreted on the basis of the sintering model by Kingery [8,9]: according to his model, the various sintering stages can be identified through a logarithmic plot of shrinkage vs. time, where the relationship for the first stages

$$\Delta L/L_0 = Kt^n \tag{1}$$

becomes

$$\Delta L/L_0 = Kt^{1/n} \tag{2}$$

for the following ones. The rate-governing step for each stage can be identified by n or $1/n$ values.

As shown in Fig. 4 different sintering stages are defined each of them characterized by different

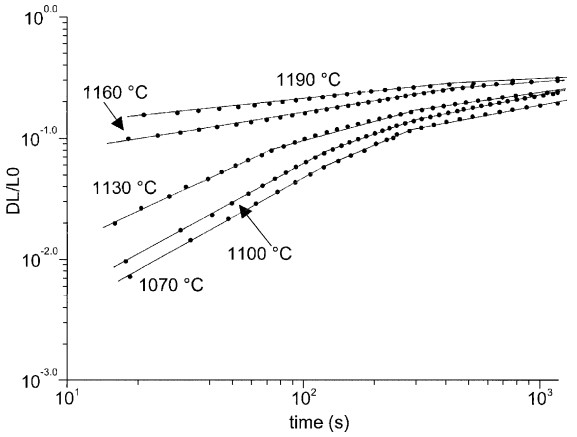

Fig. 4. Log–log plot of MgB_2 shrinkage vs. time during hot-pressing.

mechanisms depending on sintering temperature and time: Table 2 shows the n and $1/n$ values obtained for each stage.

In sample treated at 1100 °C it is possible to recognize a first stage characterized by a slope with n near to 1 which indicates a mechanism of sliding and fragmentation of the particles (Fig. 4).

At $T = 1130$ °C n value becomes <1 and that is in agreement with a process of breaking of particles necks which follows the sliding process and it is allowed only by a sufficiently high temperature. The slope of the first stage for $T = 1070$ °C is almost parallel to the one at 1130 °C: the reason could be attributed to the Mg sublimation which at this temperature is still limited and does not oppose to the neck rupture.

In the case of the curves obtained at 1070 and 1100 °C the second densification stage starts at about 120 s: the value of n obtained by (1) is definitely lower than 1; at the same time the value of $1/n$ extracted by (2) is $\approx$1/1.5 which does not reach the value of 1/2 indicating a dissolution mechanism. This stage can be considered the result of two overlapping processes which control the kinetics limiting step of densification [11]: the rearrangement proceeds while dissolution–precipitation processes starts.

For the curve recorded at $T = 1130$ °C a second stage starts at about 74 s and shows slopes with $1/n = 1/2$ indicating the solution of globular particles in a liquid intergranular phase as the rate-governing step. Actually Mg vapors can be supposed to act as a fluid under the action of the applied pressure and the dissolution of ions into the fluid to be the rate limiting step.

SEM images of fractured samples (Fig. 5a–c) show rounded grains not well crystallised, a microstructure very different indeed from that of the starting powder (Fig. 1): Mg sublimation have the effect to round off the initially prismatic MgB_2 particles, and the fluid formed on grains surface may enhance the particle sliding, at the earlier stage of densification. At this stage an equilibrium holds between the Mg sublimation from existing grains and the formation of new MgB_2 particles, due to the Mg precipitation; Fig. 5a–c shows small spots of $\sim$100–200 nm size which are nucleation centres for these new MgB_2 grains. It is interesting to note that nucleation is well visible starting from 1100 °C and increases at 1130 °C while at 1070 °C it seems almost absent: such a finding could be the reason of the higher densification extent of the 1070 °C sample at the end of the heating up before the starting of the isothermal regime. Actually if surface energy is spent for the formation of new nuclei instead of secondary recrystallisation, grain coalescence could be reduced and the neoformed nuclei on the particle surface alter surface curvature and limit free surface energy driving densification process [12]. The change in slope, after the second stage, (over 300 s) led to a $1/n$ value $\approx$1/3 (Table 2) which suggests a diffusion process to be the rate-governing step (this is true when microstructure is formed by globular particles).

Table 2
n and $1/n$ values of hot-pressed MgB_2 samples

Sintering stage	1070	1100	1130	1160	1190
Initial	$n = 1.10$	$n = 1.08$	$n = 0.90$	–	–
Intermediate	$1/n = 0.70$	$1/n = 0.67$	$1/n = 0.55$	$1/n = 0.31$	$1/n = 0.28$
Final	$1/n = 0.31$	$1/n = 0.34$	$1/n = 0.29$	$1/n = 0.15$	$1/n = 0.13$

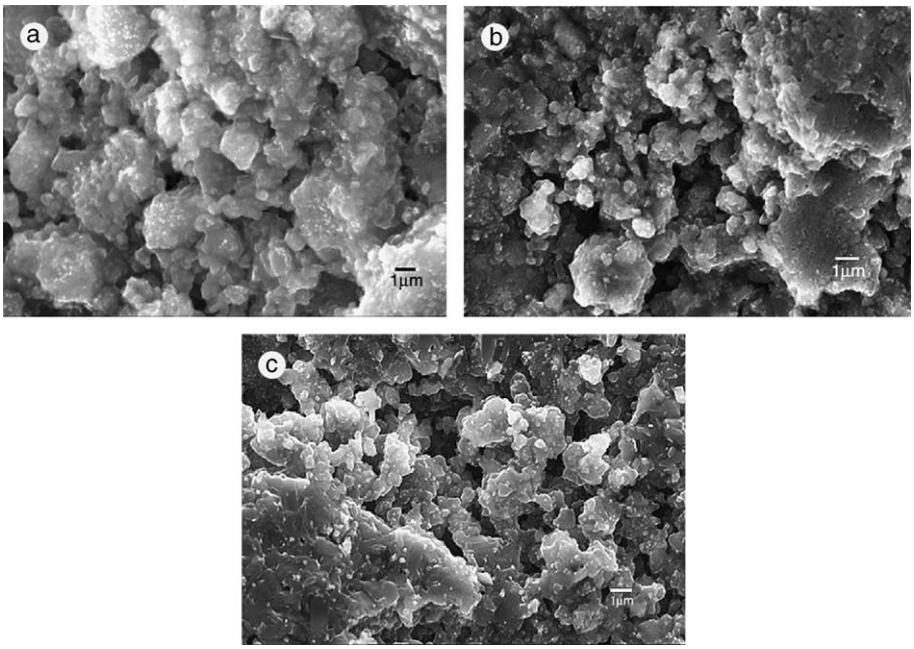

Fig. 5. SEM images of fracture surface of samples hot-pressed: (a) 1070 °C, (b) 1100 °C and (c) 1130 °C.

As densification proceeds with time, pores volume reduces increasing the vapor tension on the intergranular fluid, that moves the equilibrium $Mg_{gas} \Rightarrow Mg_{liq}$ towards the liquid state and increases the interactions inside the fluid itself which, in this condition, increases its solvent capability [13]. Thus ions dissolution becomes rapid while their diffusion into the intergranular fluid results the factor limiting the densification process. To summarize once sliding and rearrangement of particles has occurred, densification is controlled by a dissolution process of the solid matter, with a maximum value of solubility where grains are in contact, because of the highest stress zone, subsequently diffusion of ions into the liquid and a reprecipitation at zones where stress is somewhat lower becomes the mechanism of the rate limiting step. This determines an approach of the grains and the consequent densification. The sample treated at 1130 °C has an intermediate morphology and the globular grains tend to transform in more prism-like structure, similar to those of samples densified at higher temperature.

As regards the application of Kingery's model at the densification curves recorded at $T = 1160$ and 1190 °C it is possible to verify the disappearance of the rearrangement stage and the first stage has a slope with $1/n = 1/3$ which indicates a mechanism of solution of prismatic particles for the rate-governing step. The second stage starts at about 430 s (relative density ≈90%) and $1/n$ becomes 1/6 and 1/8 for 1160 and 1190 °C samples respectively. The value of 1/6 is very near to the theoretical one (1/5) for a mechanism of diffusion of prismatic particles into the intergranular liquid phase as the rate-governing step. The increase of temperature up to 1190 °C surely reduces the viscosity of the fluid phase which causes an increase in the diffusion rate, therefore in the first stage of densification, the dissolution of prismatic particles is the mechanism of the rate-governing step ($1/n = 1/3$). In the second densification stage $1/n = 1/8$ can be justified on the basis of an excessive grain growth (detectable by SEM image in Fig. 6) yielding a slowing down in the densification rate. SEM analysis of polished surfaces of hot-pressed samples (Fig. 6a and b) show that at $T = 1160$ °C macroporosity reduces drastically and at $T = 1190$ °C grain growth becomes huge.

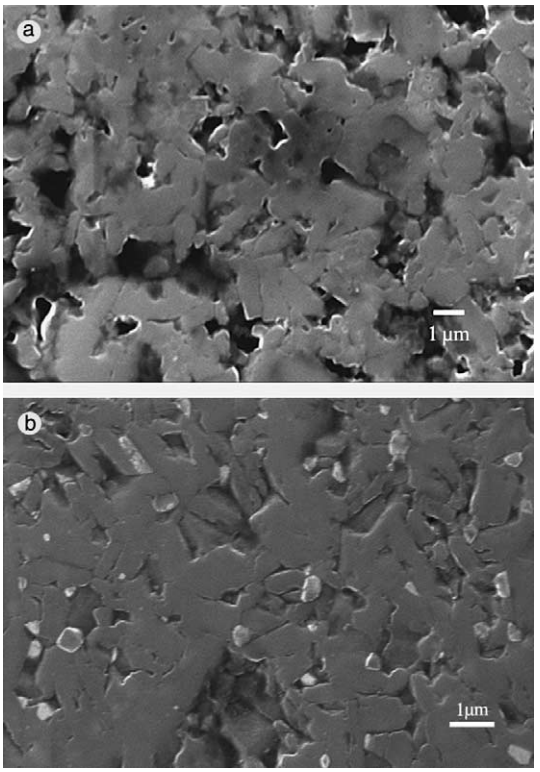

Fig. 6. SEM images of thermally etched polished surfaces of sample hot-pressed at (a) 1160 °C and (b) 1190 °C.

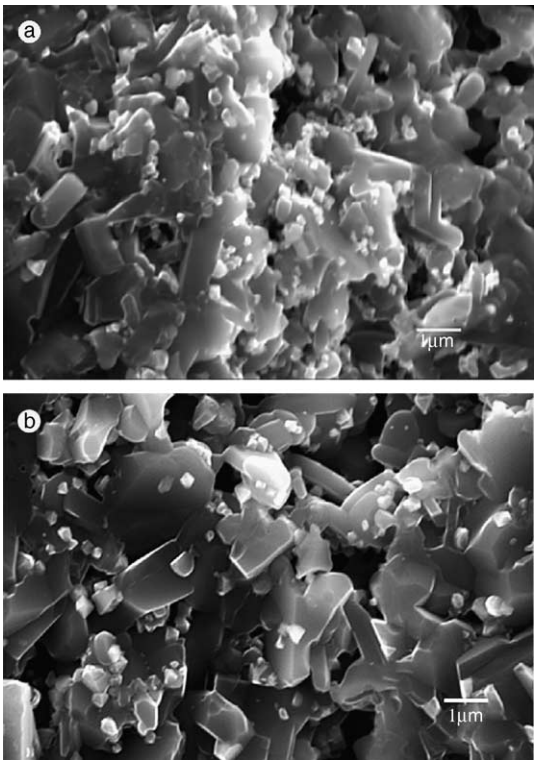

Fig. 7. SEM images of fracture surface of samples hot-pressed: (a) 1160 °C and (b) 1190 °C.

SEM images of fractured surface of 1160 and 1190 °C samples (Fig. 7a and b) show well-crystallised and elongated grains with ~1–2 μm of length and a very sharp microstructure, in comparison with low-T sintered samples. Small particles of 100–200 nm size were found between the MgB_2 grains.

The relative densities of the final samples, measured by Archimede's technique, are reported in Table 3, starting from a green relative density of about 57%, it is recorded a progressive increase of density raising the hot-pressing temperature. At T over 1160 °C this effect of temperature becomes weak and at $T = 1190$ °C the increase of relative density is less than the expected one, probably due to the opposite effect of Mg sublimation and the raised grain growth rate.

AC susceptibility measurement was carried out on sintered pieces and real (χ') and imaginary (χ'') part were evaluated and plotted vs. temperature (Fig. 8).

Table 3
Relative densities of hot-pressed MgB_2 samples

	T (°C)				
	1070	1100	1130	1160	1190
R_1	68	67	71	73	80
R_2	72	71	76	80	82
R_3	77	78	82	90	90
R_f	84	86	91	94	95

R_1: relative density at the beginning of the isothermal run; R_2: relative density at the beginning of the intermediate stage; R_3: relative density at the starting of the final stage; R_f: final relative density.

The superconducting transitions are sharp and one-step, without any kink or shoulder, confirming the bulk nature of superconductivity in dense MgB_2. χ'' curves exhibit only a single peak, sustaining the hypothesis of the absence of any secondary superconductive phase. The slight decrease of shielding fraction with increasing sintering

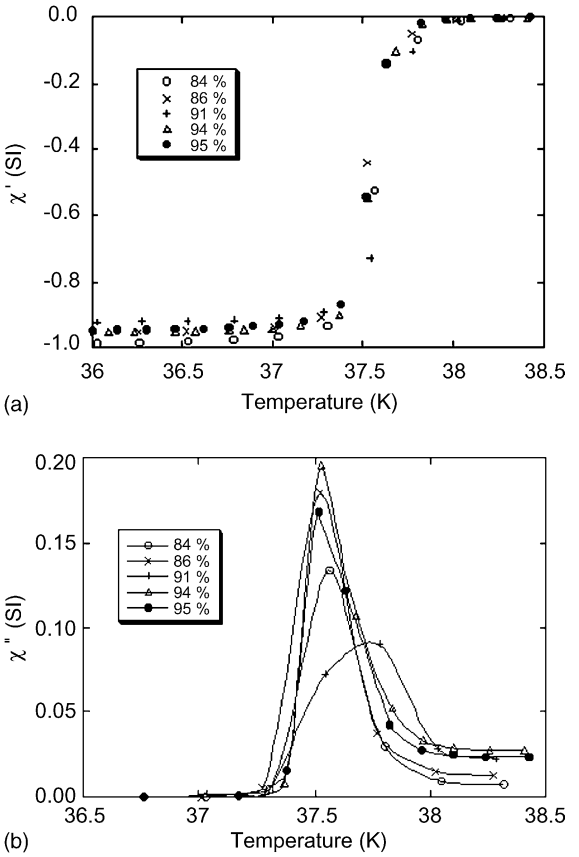

Fig. 8. Susceptibility curves of hot-pressed MgB_2 as a function of temperatures of the samples with different density. The real (a) and the imaginary (b) part of the magnetic susceptibility were collected with a driving field of 10.35 A/m oscillating at 1000 Hz.

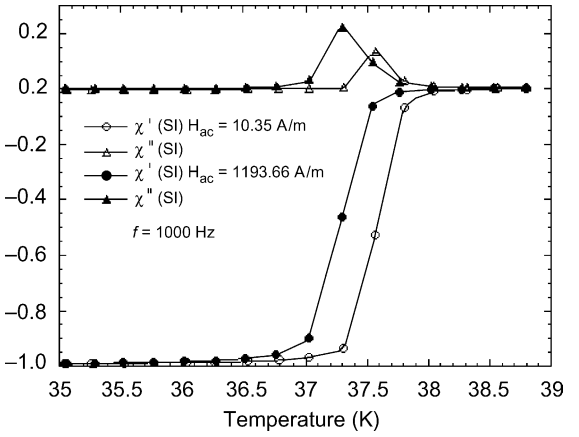

Fig. 9. χ' and χ'' vs. the temperature for the sample hot-pressed at 1070 °C with $d = 84\%$, measured with $H_{ac} = 10.35$ A/m and $H_{ac} = 1193.66$ A/m.

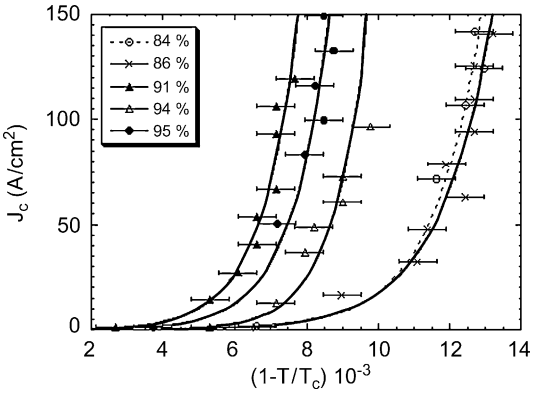

Fig. 10. The critical current density J_c vs. the normalized temperature. The lines are only guide for the eyes.

temperature may be related to the residual Mg, which remains trapped into the inner pores after the thermal treatment, forming MgO.

The onset of diamagnetism starts at about $T_c = 37.8$ K for the sample treated at 1070 °C ($d = 84\%$). As the treatment temperature increases, T_c onset value seems to gradually decrease but it does not vary appreciably.

As the measuring field increases (from 10 up to 1200 A/m), T_c and the temperature of full field penetration (the peak in χ'') decrease of about 0.3–0.5 K in all the samples. In Fig. 9, as an example, is shown the case of the sample hot-pressed at 1070 °C with $d = 84\%$.

To best characterize the samples as a function of treatment temperature (i.e. the actual density), we evaluated the critical current density (J_c) using the susceptibility data in the framework of the Bean model [14,15]. This method is based on the full penetration of the magnetic field in the sample as a function of temperature and applied field. In Fig. 10 the J_c from the different samples is depicted as a function of $(1 - T/T_c)$ [16]. It is proper to outline that, owing to the restricted range of values (the variation of the temperature of full field penetration with the field is small) and the experimental noise, it is not possible to fit the data and extrapolate J_c values at low temperature in a

reliable way. So the line in the figure are only a guide for the eyes, even if the application of an usual quadratic extrapolation to lower temperature yields the values already reported in the literature [2]. Despite to this fact, the data seem to claim the existence of two different types of samples and those with $d > 90\%$ seem to produce the better results in term of critical current.

4. Conclusions

The sintering behaviour of MgB_2 was studied by means of isothermal hot-pressing experiments at different temperatures on commercial MgB_2 powder. Densification has been found to start at temperatures ≈1050 °C and it begins to be hampered by an effective grain growth at temperatures higher than 1160 °C, reaching a final relative density ≈95%. The secondary phases formation is nearly independent on the sintering temperature, anyway susceptibility measurements show that raising the sintering temperature a decrease of the shielding fraction occurs, caused by residual Mg trapped into pores. The study of densification behaviour by means of Kingery's model for liquid phase sintering reveals that, after a first stage of grain sliding and fragmentation, an ion dissolution with subsequent diffusion process and recrystallisation occurs, suggesting that Mg, which is sublimated at working temperatures, may act as a fluid which enhances the matter transport. The same Mg however, at the latest stage of sintering, is trapped into closed pores and becomes MgO after the sample cooling, preventing the complete densification. Densification processes carried out at $T = 1160$–1190 °C are controlled by different mechanisms since diffusion is the rate-governing step in the first stage (probably solubility is strongly enhanced in the low-viscosity fluid). After 13–16 min of densification, dissolution of prismatic grains becomes the rate-governing step: this last period of densification is the main responsible of secondary phases recrystallisation. Therefore to prevent recrystallisation of secondary phases the best hot-pressing temperature is located around 1150–1160 °C even if sintering time could be reduced at 13–15 min.

In this conditions ac magnetic susceptibility measurements show that samples are still of good quality, presenting a sharp superconducting transition; moreover all samples seem to support high critical current even though it is not possible to extrapolate a value at low temperature (typically 30 and 5 K). The different values of J_c in the hot-pressed samples can be explained in terms of intergranular links. The increasing density with hot-pressing temperature tends to induce a better connectivity between grains and, despite of the secondary phases recrystallisation phenomenon, the critical current density increases.

References

[1] J. Nagamatsu, N. Nakagawa, T. Muranaka, Y. Zenitani, J. Akimitsu, Nature 410 (2001) 63.
[2] D.C. Larbalestier, L.D. Cooley, M.O. Rikel, A.A. Polyanskii, J. Jiang, S. Patnaik, X.Y. Cai, D.M. Feldmann, A. Gurevich, A.A. Squitieri, M.T. Naus, C.B. Eom, E.E. Hellstrom, R.J. Cava, K.A. Regan, N. Rogado, M.A. Hayward, T. He, J.S. Slusky, P. Khalifah, K. Inumaru, M. Haas, Nature 410 (2001) 186.
[3] M. Kambara, N. Hari Babu, E.S. Sadaki, J.R. Cooper, H. Minami, D.A. Cardwell, A.M. Campbell, I.H. Inoue, Supercond. Sci. Technol. 14 (2001) L5.
[4] D. Hinz, A. Handstein, G. Fuchs, K.-H. Müller, K. Nenkov, O. Gutfleisch, V.N. Narozhnyi, L. Schultz, Physica C 372–376 (2002) 1248.
[5] Y. Takano, H. Takeya, H. Fujii, H. Kumakura, T. Hatano, K. Togano, H. Kito, H. Ihara, Appl. Phys. Lett. 78 (2001) 2914.
[6] C.U. Jung, M.S. Park, W.N. Kang, M.S. Kim, K.H.P. Kim, S.Y. Lee, S.I. Lee, Appl. Phys. Lett. 78 (2001) 4157.
[7] T.C. Shields, K. Kawano, D. Holdom, J.S. Abell, Supercond. Sci. Technol. 15 (2002) 202.
[8] W.D. Kingery, J. Appl. Phys. 30 (1959) 307.
[9] W.D. Kingery, J.M. Woulbroun, F.R. Charvat, J. Am. Ceram. Soc. 46 (1963) 391.
[10] P. Duhart, Ann. Chim. 7 (1962) 339.
[11] A.L. Prill, H.W. Hayden, J.H. Brophy, Trans. Metal. Soc. 233 (1965) 960.
[12] W.D. Kingery, H.K. Bowen, D.R. Uhlmann, Introduction to Ceramics, John Wiley and Sons, New York, 1976, p. 448ff.
[13] D.W. Matson, R.J. Smith, J. Am. Ceram. Soc. 72 (1989) 871.
[14] F. Gomory, P. Lobotka, Solid State Commun. 66 (1988) 645.
[15] A. Buekenhoudt, H. Weyten, P. Devos, F. Servaes, J. Cornelis, J. Alloys Compd. 195 (1993) 177.
[16] J. Jung, I. Isaac, M.A.-K. Mohamed, Phys. Rev. B 48 (1993) 7526.